Gas Interchange between a Bubble and Continuous Phase in Gas-Soild Fluidised Bed

By

Ryozo TOEI* and Ryuichi MATSUNO*

(Received June 27, 1968)

The mechanism of gas interchange between a bubble and the continuous phase was investigated by blowing a bubble of visible brown NO_2 gas into two dimensional fluidised bed. From this investigation, it was found that the gas interchange occurred by the diffusion and by the flow out of gas from the cloud which was caused by variations of velocity and diameter of bubble.

Based on the above transfer mechanism, a model for gas interchange was suggested and the gas interchange coefficient was calculated. Furthermore, gas interchange coefficients were obtained by measuring the change of the concentration of a CO_2 gas bubble at two different heights in the bed. The gas interchange coefficients calculated from the model coincided well with that obtained from experiments.

1. Introduction

The gas interchange between the bubbles and the continuous phase has the important effects on the various operations in gas-solid fluidised bed. The rate of gas interchange was measured by Kobayashi et al.[1] and Lewis et al.[2] from the residense time distribution of gas and the conversion based on the two phase theory or modified two phase theory.

Furthermore Szekely[3] and Richardson et al.[4] measured the gas interchange coefficient from the amount of tracer gas left in the continuous phase and the change of concentration of tracer gas in the continuous phase by blowing the bubbles of tracer gas into the bed one after another with the regular time interval.

Rowe et al.[5] blew a visible brown NO_2 gas bubble into the two dimensional fluidised bed and investigated the behaviour of NO_2 gas around the bubble. From that investigation, they found that NO_2 gas in the cloud was shed out from the cloud in discrete amounts and it formed a characteristic "Christmas tree" pattern below the bubble.

* Department of Chemical Engineering

The authors blew a NO_2 gas bubble into the two dimensional fluidised bed of minimum fluidised state as Rowe et al. did and observed the behaviour of the gas interchange. Based on this observation a model for the gas interchange was suggested and the gas interchange coefficient was calculated.

A CO_2 gas bubble was blown into a two dimensional fluidised bed and a small amount of gas was sucked from a bubble at each of two points on the vertical direction when a bubble passed through these two points. The change of concentration of CO_2 gas in a bubble was measured. From this experiments, the gas interchange coefficient was obtained and it was compared with the calculated one from our model. These two coincided fairly well with each other.

2. Experimental procedures

A two dimensional fluidised bed (width 40 cm, height 130 cm and thickness 2 cm) made of transparent acrylic resin was used as a fluidised bed apparatus and a packed bed (height 8 cm) of 65~80# glass beads was used as the calming part of the fluidising air. On the experiments blowing a NO_2 gas bubble to the fluidised

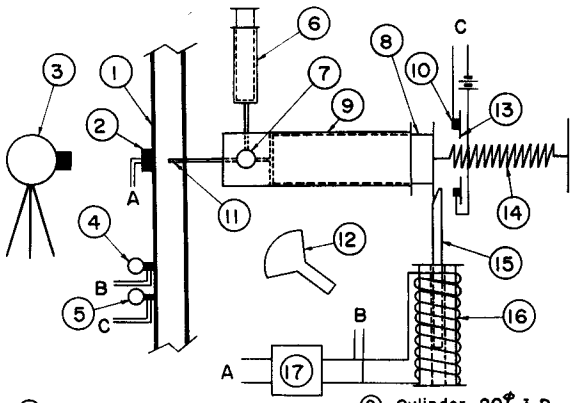

Fig. 1 Schematic diagram of sampling section.

bed, to make the colour of NO_2 gas most brown, the whole apparatus was set in the chamber of 50°C and the fluidising air was dehumidified through the packed bed of silica gel. A NO_2 gas bubble was blown into minimum fluidising bed through a nozzle installed at the bottom of the bed by an electro magnetic valve. The motions of a NO_2 gas bubble and of NO_2 gas in the dense phase were photographed by a 16 mm cine camera (32 frame/sec) and were analysed by film analyser. The glass beads of 42～48# and 80～100# were used as fluidising particles.

As same as the above procedure, a CO_2 gas bubble was blown into the minimum fluidising bed through a nozzle by an electro magnetic valve. A small amount of gas within the CO_2 gas bubble was sampled at two points on the vertical line (heights from nozzle were 40 cm and 70 cm) just when the bubble passed through at each point and the concentrations of CO_2 gas were measured by a gas chromatograph. The schematic diagram of sampling section was shown in Fig. 1. When a bubble reached the sampling section, the photo transistor ② caught the light of photo reflector lamp transpierced through the two dimensional bed and the relay ⑰ was set to work. The stopper ⑮ of piston ⑧ of cylinder ⑨ was removed by the electro magnet which was connected to relay and the gas was sucked rapidly into the cylinder. Th sampling volume was ca. 2～3cc and the sampling time was 1/24 sec. The lamps ④ and ⑤ were lighted at the beginning and the finish of the sampling respectively, so the sampling time could be checked.

The sampled gas was led to the sampler tube ⑥ for gas chromatography through the three ways cock ⑦ by pushing the piston ⑧.

During this experiment, the whole of the fluidised bed was photographed by 16 mm cine camera (48 frame/sec) with back light and the size and rising velocity of a bubble were measured. Furthermore it was checked whether the sampling was performed in the bubble correctly or not.

The glass beads of 24～28#, 42～48#, 60～65# and 80～100# were used as fluidising particles.

3. Experimental results by a NO_2 gas bubble and the model for the gas interchange.

3–1 Experimental results by a NO_2 gas bubble

The behaviour of NO_2 gas when a NO_2 gas bubble passed through the fluidising bed was almost the same as that of Rowe et al.'s[5]. An example was shown in Photo. 1.

The results were summarised as follows.

1. The cloud was formed around the bubble. The size of the cloud for the

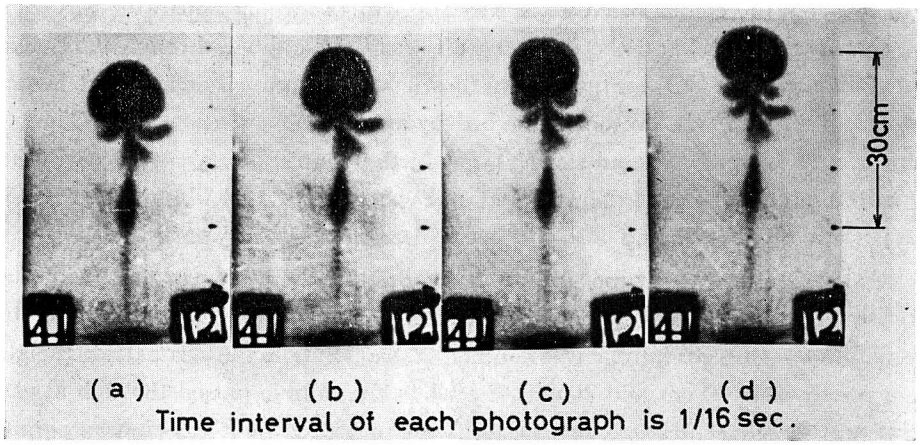

Photo. 1 Behavior of NO_2 gas around a bubble. (42～48# glass beads)
(Time interval of each photograph is 1/16 sec.)

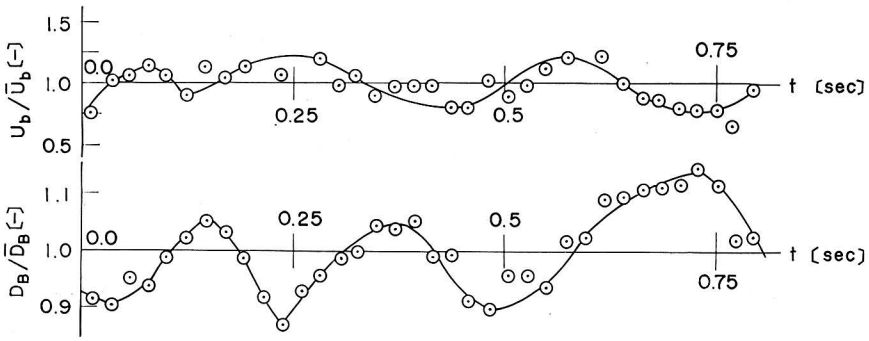

Fig. 2 An example of variation of velocity and diameter of bubble.
(60～65# glass beads bed)

same bubble size was larger for the 42～48# glass beads bed than for the 80～100# glass beads bed. The value of α for the former was smaller than for the latter.

2. As shown in Photo. 1, NO_2 gas in the cloud was shed out from the cloud and it formed a characteristic "Christmas tree" pattern below the bubble.

3. The average frequencies of shedding out of NO_2 gas from the cloud were ca. 3 times/sec for the 42～48# glass beads bed and ca. 6～8 times/sec for the 80～100# glass beads bed. The frequencies for the 80～100# glass beads bed were ca. twice as much as that for 42～48# glass beads bed. So, in the 80～100# glass beads bed, it seemed as if NO_2 gas flew out from the cloud continuously.

4. The amount of NO_2 gas flowed out to the 80～100# glass beads bed was much more than that to the 42～48# glass beads bed.

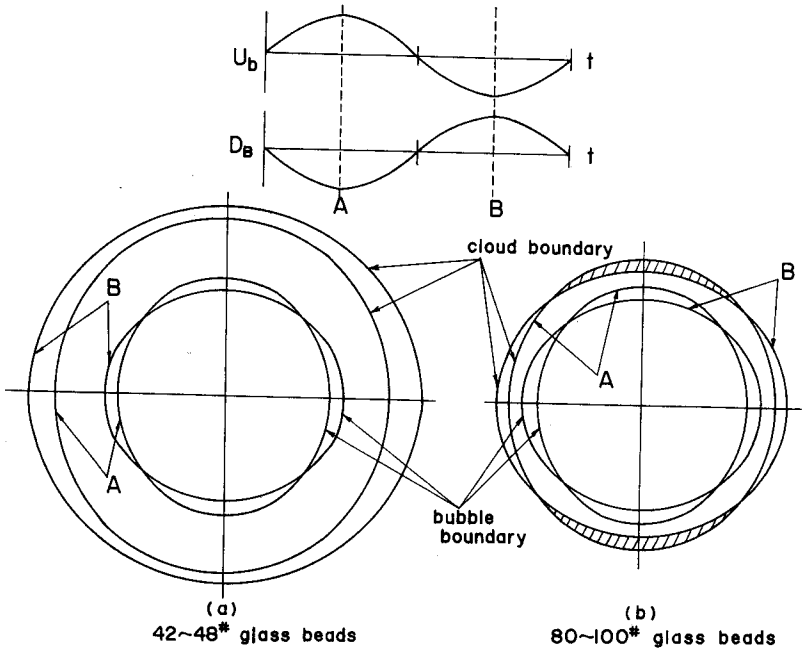

Fig. 3 Qualitative illustration of variation of cloud caused by the change of velocity and diameter of bubble.
(a) 42~48# glass beads (b) 80~100# glass beads

The state how NO_2 gas was shed out from the cloud was observed carefully on the film analyser and it could be concluded that the shedding out of gas from the cloud occurred when the rising velocity of a bubble became larger. The rising velocity and the width of a bubble were measured on the film analyser also and an example of results was shown in Fig. 2.

As shown in Fig. 2, th rising velocity of a bubble changed periodically when a bubble passed through the bed. Furthermore the width of a bubble became smaller as the rising velocity became larger and larger as the rising velocity became smaller.

The shape of bubble elongated when the width of bubble became smaller and flattened when larger.

From the above experimental results and the stream function of the gas around the bubble which was obtained by Davidson[6], the mechanism of the shedding out of gas from the cloud could be described qualitatively as follows.

Davidson's equation is

$$\psi_f = (U_b - u_0)\sin\theta \cdot r - \frac{(U_b + u_0)a^2 \sin\theta}{r} \qquad (1)$$

When the rising velocity becomes smaller, the cloud becomes larger as calculated from Eq. (1) and as shown B in Fig. 3 (a). So the gas within the average cloud flows outside and the cloud expands as shown in Photo. 1(b).

When the velocity becomes larger, the cloud becomes smaller as shown A in Fig. 3(a). At that time the gas of the expanded part of Photo. 1(b) is cut off as shown in Photo. 1(c) and (d) and left behind the bubble. The change of the bubble width promotes this effect furthermore.

In the above description, the average cloud means the circle which is obtained from Eq.(1) when the rising velocity is equal to the average one.

Approximating the variation of rising velocity and width of a bubble as sine curve, the ratios of maximum value of variating portion to the average value were obtained using the standard deviation. The average values of the ratios, K, for the rising velocity and those, K', for the width of bubble were 0.2 and 0.07 respectively.

It could not be made clear why the variations of the rising velocity and the width of a bubble occurred.

As mentioned above, it can be concluded that the gas interchange between a bubble and a desne phase occurred by the shedding out of gas from the cloud by the variations of the rising velocity and of the width of bubble, and also by the diffusion of gas from the cloud around the bubble.

But as it is very difficult to deal with the shedding out of gas from the cloud and the gas diffusion together, each phenomenon was analysed individually by each model. The gas interchange coefficients were calculated for these two and the total gas interchange coefficient was assumed to be the sum of these two coefficients.

3–2 Model for the shedding out of gas from the cloud.

For the shedding out of gas from the cloud, the following model was suggested.

It is assumed that the rising velocity and width of bubble vary as sine curve as shown in Fig. 3 and that the shape of bubble becomes an elongated or flattened ellipse whose area is equal to that of the average bubble.

The gas stream function Eq.(1) which was obtained by Davidson[6] is extended to this case.

The complex potential F equivalent to Eq.(1) is as follows.

$$F = \phi_f + i\Psi_f = (U_b - u_0)z + \frac{(U_b + u_0)a^2}{z} \tag{2}$$

where

$$U_b = \bar{U}_b(1 + K \sin 2\pi\lambda t) \tag{3}$$

The symbol λ means the frequency of variation of rising velocity or width of bubble and is ca. 3 times/sec from the experimental results.

Eq.(2) and (3) indicate the flow which is taken into account the variation of rising velocity.

To consider the transformation of bubble to an ellipse, Eq.(2) should be transformed to the flow around the ellipse by using Eq.(4) of the conformal transformation function to ellipse.

$$\zeta = z+P/z \tag{4}$$

A certain size of ellipse in ζ plane corresponds to a cirele of radius a' in z plane. The apex of circle of radius a' and the point at 90 degree from the apex on the circle in z plane corresponds to Eq.(5) and (6) in ζ plane respectively.

$$a'+P/a' \tag{5}$$

$$a'-P/a' \tag{6}$$

When P is positive, Eq.(5) and (6) show a half of the long and short axes respectively and when P is negative, the inverse relation is held. As it was assumed that the area of ellipse was equal to that of the average bubble of radius a, the next relation must be held.

$$\pi a^2 = \pi(a'+P/a')(a'-P/a') \tag{7}$$

As a half of the width of the elliptic bubble is equal to Eq.(6), the following equation can be obtained.

$$a(1-K'\sin 2\pi\lambda t) = (a'-P/a') \tag{8}$$

From Eq.(7) and (8), a' and P are calculated. As K' is small, a' is nearly equal to a and P is expressed by Eq.(9).

$$P = \frac{a^2}{4}\left[\frac{1}{(1-K'\sin 2\pi\lambda t)^2}-(1-K'\sin 2\pi\lambda t)^2\right] \tag{9}$$

As P and a' are decided as above, the complex potential around the ellipse is obtained by solving Eq.(4) with respect to z and substituting it in Eq.(2).

$$\begin{aligned} F = \phi_f+i\phi_f &= (U_b-u_0)(\zeta+\sqrt{\zeta^2-4P})/2 \\ &+2(U_b-u_0)a^2/(\zeta+\sqrt{\zeta^2-4P}) \end{aligned} \tag{10}$$

From Eq.(10), the stream function ψ_f of the gas around the ellipse is obtained as follows.

$$\begin{aligned} \psi_f &= (U_b-u_0)\{\rho\sin\beta+[Q-(\rho^2\cos 2\beta-4P)]^{1/2}/\sqrt{2}\}/2 \\ &-2(U_b-u_0)a^2\{\rho\sin\beta+[Q-(\rho^2\cos 2\beta-4P)]^{1/2}/\sqrt{2}\}/S \end{aligned} \tag{11}$$

$$Q = [(\rho^2 \cos 2\beta - 4P)^2 + \rho^4 \sin^2 2\beta]^{1/2} \tag{12}$$

$$S = \rho^2 + Q + \sqrt{2}\,\rho \sqrt{\cos^2\beta}[Q + (\rho^2 \cos 2\beta - 4P)]^{1/2} + \sqrt{2}\,\rho \sin\beta[Q - (\rho^2 \cos 2\beta - 4P)]^{1/2} \tag{13}$$

As the gas-flow outside the bubble is considered, P is far smaller than ρ^2 and Eq.(11) is reduced as Eq.(14).

$$\psi_f = (U_b - u_0)\sin\beta \cdot \rho(1 + P/\rho^2) - \frac{(U_b + u_0)a^2 \sin\beta}{\rho}\left[1 + \frac{P}{\rho^2}(1 + 2\cos 2\beta)\right] \tag{14}$$

This stream function varies periodically, but the inertia of particle motion is not considered.

Fig.3(a) and (b) showed qualitatively the bubble boundary and cloud boundary at the states of A and B of upper figure of Fig. 3 refered to Eq.(14). The cloud boundary in the figure shows the position where $\psi_f = 0$ in Eq.(14).

When the particle size is large and α is small the cloud boundary of state B is larger than that of state A as shown in Fig.3(a). When the particle size is small and α is large, the cloud boundaries of the state A and B intersect each other as shown in Fig.3(b).

As mentioned in section 3–1 that the shedding out of gas from the cloud occurred when the rising velocity of bubble became large, gas of the expanded portion is cut off when the rising velocity becomes large in both cases of Fig.3(a) and (b). In the case of (b), the upper and lower sections of the cloud are expanded by gas flowed out from inner side as shown in Fig.3(b) at that time. And then when the rising velocity becomes small, the gas of that expanded portion is shed out. That is, the shedding out of gas from the cloud should occure two times during one cycle of the variation of the rising velocity and width of bubble.

From the above reason, the experimental result metnioned in 3–1, that is the frequency of the shedding out of gas from the cloud to 80～100# glass beads bed was almost twice as much as that to 42～48# glass beads bed, can be explained.

The positions relative to the center of bubble of the gas elements whose initial positions were on the average cloud boundary were calculated numerically during one cycle of the variation of the velocity and width of bubble by using Eq.(14) and the drift line of the average cloud surface after one cycle was obtained by linking the final positions of the gas elements. It was shown in Fig.4 with mark A.

Although λ was ca. 3 times/sec, it was taken 3.125 times/sec for the convenience of the calculation. From Fig.4, the characteristic "Christmas tree" pattern can be explained and the flow of gas into and out of the average cloud is found.

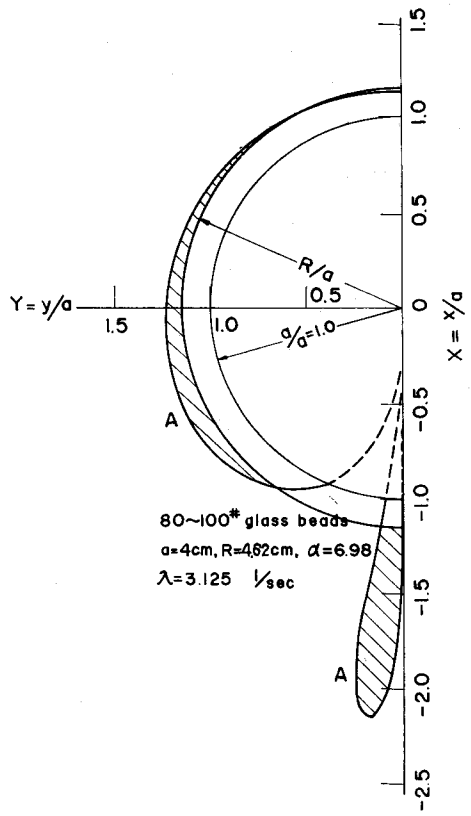

Fig. 4 Drift line of cloud surface after one cycle of variation of velocity and diameter of bubble.

As Fig.4 is symmetrical about X axis, the double amount of the hatched area A_{out} multiplied by voidage fraction is the amount of the gas interchange per one cycle of variation.

The gas interchange corefficient k_{gc} based on the suface area of the bubble was obtained by the next mass balance.

$$k_{gc}\pi\bar{D}_B(c_0-0)=\frac{\varepsilon_{mf}}{1+2\varepsilon_{mf}/(\alpha-1)}\cdot\lambda A_{out}(c_0-0)$$

$$k_{gc}=\frac{1}{1+2\varepsilon_{mf}/(\alpha-1)}\cdot\frac{\varepsilon_{mf}A_{out}\lambda}{\pi\bar{D}_B} \tag{15}$$

It was assumed that the concentrations of the cloud and bubble were the same. The value of k_{gc} was obtained from the amount of gas flown out from the cloud by Eq.(15). But as described above, k_{gc} is defined as [cm³-gas/sec cm²-bubble surface], the first term of the right hand side of Eq.(15), $1/\{1+2\varepsilon_{mf}/(\alpha-1)\}$, should

be multiplied as volume correction factor.

Since A_{out} and the volume correction factor decrease with the decrease of α, the value of k_{gc} decreases with the decrease of α, that is, with the increase of the particle size and the decrease of bubble diameter.

3–3 Gas interchange by diffusion

Davidson et al.[6] obtained the gas interchange coefficient between bubble and dense phase by diffusion. The coefficient k_{gd} of the gas interchange from the surface of the cloud by diffusion was calculated by almost the same way as Davidson et al.'s.

Taking the co-ordinate near the cloud surface as shown in Fig. 5, a small element ABCD is considered.

As the gas stream line near the cloud surface is considered almost to be parallel to AC and BD except near $\theta=0$ or π, it can be assumed that the gas is transfered through AC and BD only by diffusion but not by concvetive flow.

The convective flow governs the gas transfer through AB and CD and the gas diffusion can be neglected. The following partial differential equation is derived.

$$D_G R\left(\frac{\partial^2 c}{\partial s^2}\right)_\theta = v_G\left(\frac{\partial c}{\partial \theta}\right)_s \tag{16}$$

The symbol v_G is the gas velocity through AB and is the function of θ. Considering s is small compared with the radius of the cloud near the cloud surface, Eq.(1) is linearlized as follows.

$$\psi_f = 2u_0(\alpha-1)s\cdot\sin\theta \tag{17}$$

In this equation, the opposite sign is used for ψ_f against that of Eq. (1).

From Eq.(17), v_G can be obtained.

The boundary conditions are taken as follows.

at $s=0$ $(\psi_f=0)$, i.e. at cloud surface, $c=c_0$

at $s=-\infty$ $(\psi_f=0)$, $c=c^*=0$

To convert Eq.(16) to the form of the standard diffusion equation, the variable Θ defined by Eq. (18) is introduced.

$$d\Theta/d\theta = 2Ru_0(\alpha-1)\sin\theta \tag{18}$$

From Eq.(17) and (18), Eq.(16) can be converted to Eq.(19).

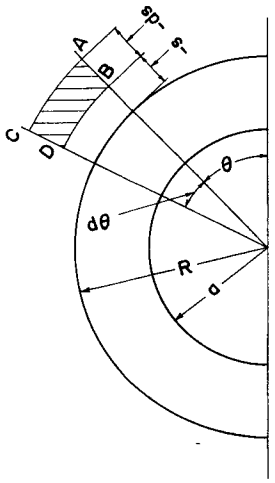

Fig. 5 Co-ordinate near the cloud surface for the calculation of k_{gd}.

$$D_G\left(\frac{\partial^2 c}{\partial \psi_f{}^2}\right)_\theta = \left(\frac{\partial c}{\partial \theta}\right)_{\psi_f} \tag{19}$$

The solution is,

$$\frac{c-c_0}{c_0} = \frac{2}{\sqrt{\pi}}\int_{-\infty}^{\eta} e^{-\eta^2} d\eta - 1, \quad \eta = \frac{\psi_f}{2\sqrt{D_G\theta}} \tag{20}$$

If the whole of the circular cloud surface works effectively, the amount of the transfered gas from the surface of the cloud is,

$$N_c = 2D_G\varepsilon_{mf}\int_0^{\pi} R\left(\frac{\partial c}{\partial s}\right)_{s=0} d\theta = 2\varepsilon_{mf}\sqrt{\frac{16D_G Ru_0(\alpha-1)}{\pi}}\cdot c_0 \tag{21}$$

From this equation, the gas interchange coefficient k_{gd} by diffusion based on the surface of bubble is obtained.

$$\begin{aligned} k_{gd} &= \frac{2\varepsilon_{mf}}{1+2\varepsilon_{mf}/(\alpha-1)}\cdot\sqrt{\frac{4D_G Ru_0(\alpha-1)}{\pi^3 a^2}} \\ &= \frac{1.02\varepsilon_{mf}}{1+2\varepsilon_{mf}/(\alpha-1)}\cdot\sqrt{\frac{\bar{U}_b D_G}{\bar{D}_B}\frac{(\alpha-1)}{\alpha}\sqrt{\frac{\alpha+1}{\alpha-1}}} \end{aligned} \tag{22}$$

The value of k_{gd} increases in proportion to the square root of diffusion coefficient. As $\bar{U}_b$ is nearly proportional to $\bar{D}_B{}^{1/2}$, k_{gd} is proportional to $\bar{D}_B{}^{-1/2}$. But when α becomes small by the increase of particle size, it becomes small with decrease of $\bar{D}_B$ because of the sharp decrease of the volume correction factor.

3–4 The total gas interchang coefficient

Although the diffusion is superimposed on the shedding out of gas from the cloud, it was assumed that these two phenomena occured individually and the total gas interchange coefficient was defined by the next equation.

$$k_{gt} = k_{gc} + k_{gd} \tag{23}$$

Furthermore it was assumed that the concentrations of cloud and bubble were same because of rapid circulation of gas between them.

Above two assumptions are introduced into our model.

4. Experimental results by a CO_2 gas bubble and comparison with the model.

The shape of bubble is assumed to be circular. From the mass balance, the next equation is derived.

$$-\frac{\pi\bar{D}_B{}^2}{4}\frac{dc}{dt} = k_{gt}\pi\cdot\bar{D}_B(c-c^*), \qquad c^* = 0 \tag{24}$$

The rising velocity of a bubble is defined as,

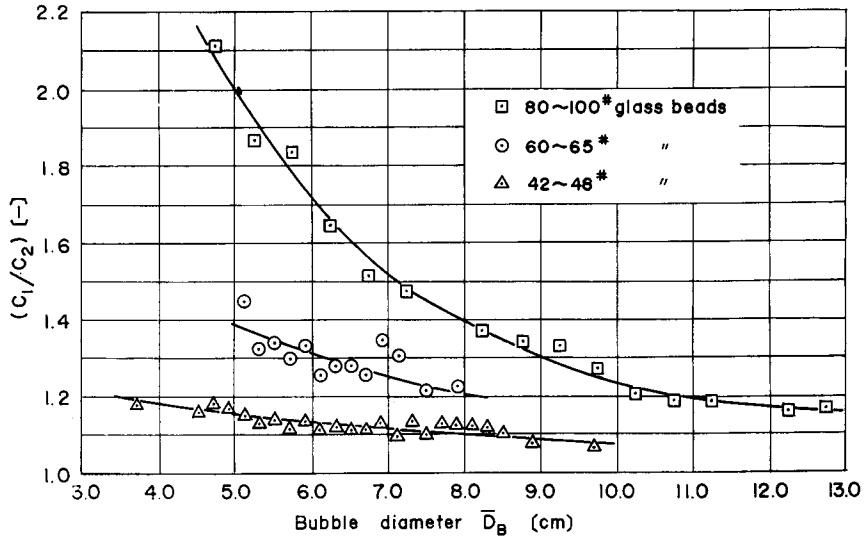

Fig. 6 Concerntrations ratio of lower and upper sampling points. (c_1 and c_2 are CO_2 gas conc. at 40 cm and 70 cm from nozzle.)

$$\bar{U}_b dt = dl \tag{25}$$

From Eqs. (24) and (25),

$$k_{gt} = \frac{\bar{D}_B \bar{U}_b}{4l} ln(c_1/c_2) \tag{26}$$

By Eq. (26), the gas interchange coefficient k_{gt} can be calculated from the experimental results.

The value of k_{gt} respect to each bubble scattered very much. The scattering of k_{gt} was especially large for 42~48# glass beads bed and it exceeded $\pm 100\%$. So the average concentration ratio (c_1/c_2) was plotted against the bubble diameter and was shown in Fig. 6. The distance of the sampling position was 30 cm. The larger the diameter of bubble and the the particle size were, the smaller the concentration ratio was.

The data when the bubble split were not contained in the above plotting. The concentration ratio increased remarkably in 42~48# glass beads bed when the bubble split. In the experiment of a NO_2 gas bubble, the flow out of gas from a bubble was recognized when the bubble split. Especially in 42~48# glass beads bed that amount was considerable. Muchi et al.[7] pointed out that the motion of gas around the bubble had an important effect on the gas interchange when the bubble coalesced or split. As mentioned above, their indication is especially important when

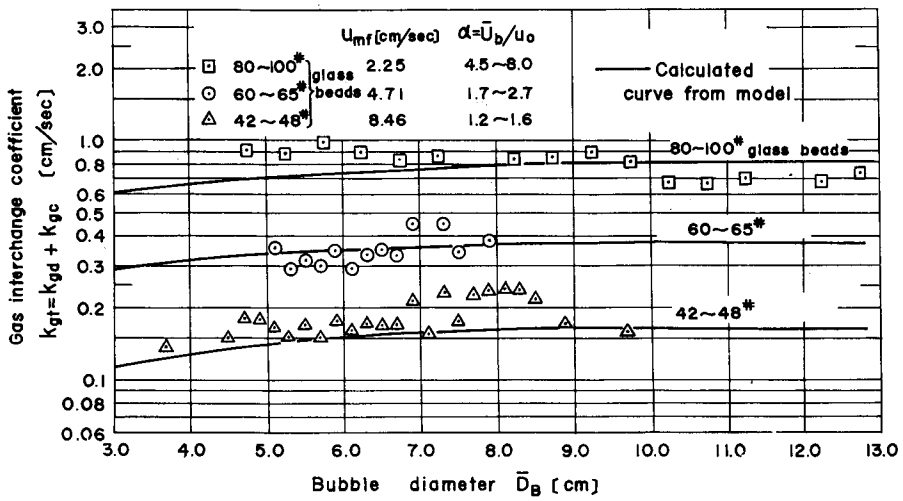

Fig. 7 Gas interchange coefficient between a bubble and continuous phase.

Table 1. Gas interchange coefficient calculated from model

Particle	$\bar{D}_B$ [cm]	α [—]	k_{gd} [cm/sec]	k_{gc} [cm/sec]	k_{gt} [cm/sec]
42~48#	3.0	1.22	0.0738	0.0388	0.113
glass beads	5.0	1.33	0.0940	0.0453	0.139
$u_{mf}=8.46$	8.0	1.43	0.106	0.0527	0.159
[cm/sec]	10.0	1.49	0.111	0.0531	0.164
60~65#	3.0	1.72	0.200	0.0999	0.300
glass beads	5.0	2.02	0.218	0.119	0.337
$u_{mf}=4.71$	8.0	2.39	0.226	0.135	0.361
	10.0	2.52	0.230	0.142	0.372
80~100#	3.0	4.66	0.350	0.268	0.618
glass beads	5.0	5.75	0.347	0.337	0.684
$u_{mf}=2.25$	8.0	6.98	0.318	0.455	0.773
	10.0	7.65	0.306	0.496	0.802

the particle size is large.

In 24~28# glass beads bed ($\alpha<1$), the concentration of CO_2 was already equal to zero at the lower sampling position. Namely, it was considered from Eq. (1) that the CO_2 gas passed through the bubble.

By using the concentration ratio of Fig. 6, k_{gt} was calculated and plotted against $\bar{D}_B$ as shown in Fig. 7. It becomes larger with increase of α.

The calculated results by our model was shown by bold line on the same figure.

They coincide farely well with each other and it can be said that our model is appropriate.

The examples of the calculated results of the model were shown in Table 1 with respect to k_{gd} and k_{gc}.

It is known from Fig. 7 and Table 1 that the gas interchange coefficient becomes smaller as the particle size larger.

The reason is condidered as follows. Although the amount of gas transfered by diffusion from the cloud surface does not differ so much with the difference of the particle size because the value $\sqrt{Ru_0(\alpha-1)}$ does not differ with the particle size, the volume correction factor of Eq. (22) becomes smaller as the particle size larger. So the gas interchange coefficient k_{gd} by diffusion becomes smaller as the particle szie larger.

It is known from Eq. (14) that the tangential gas velocity near the cloud surface is almost proportional to $(\bar{U}_b-u_0)$ for fixed β. When the rising velocity of a bubble becomes smaller and the bubble becomes flat, gas flows out crossing the average cloud boundary near the surface of the upper half of cloud. If the tangential velocity is large, that is $(\bar{U}_b-u_0)$ is large, the gas is flowed down rapidly to the out-side of the average cloud of the lower section of the bubble and most part of the gas flows out.

If $(\bar{U}_b-u_0)$ is small, gas which is flowed out from the upper section of the average cloud does not move so far and a part of the gas flows back to the average cloud when the rising velocity becomes larger and the bubble becomes elongated. So a litle amount of gas flows out as a result.

The amount of flowed out gas from the cloud becomes smaller because of the small $(\bar{U}_b-u_0)$ when the particle size and so u_{mf} are large. Furthermore the volume correction factor is small when the particle size is large. So the gas interchange coefficient k_{gc} of the large particle becomes smaller than that of smaller one.

From above reasons, the total gas interchange coefficient k_{gt} becomes smaller as the particle size larger.

5. Conclusion.

From the experiments using a NO_2 gas bubble as a tracer, the behaviour of gas interchange between the bubble and continuous phase was investigated and a model of the gas interchange was suggested. The gas interchange coefficient was calculated based on this model. On one side, the gas interchange coefficient was obtained from the experiments using a CO_2 gas bubble and was compared with the one from our model. These two coincided farely well with each other and

the experimental results could be explained by our model.

Nomenclature

A_{out}	:	area of gas which comes out from cloud after one cycle of variation of rising velocity of bubble	[cm²]
a	:	radius of bubble	[cm]
a'	:	radius of circle in z plane which coressponds to ellipse in ζ plane	[cm]
c	:	concentration of gas	[—]
c^*	:	concentration far away from cloud	[—]
c_0	:	concentration in cloud	[—]
c_1	:	concentration of lower sampling point	[—]
c_2	:	concentration of upper sampling point	[—]
D_B	:	bubble diameter	[cm]
$\bar{D}_B$	:	average bubble diameter (width)	[cm]
D_G	:	diffusion coefficient of gas	[cn²/sec]
d_p	:	particle diameter	[μ]
F	:	complex potential	[cm²/sec]
i	:	unit complex number	[—]
K	:	ratio of maximum variating portion of rising velocity to average rising velocity	[—]
K'	:	ratio of maximum variating portion of diameter of bubble to average diameter	[—]
k_{gc}	:	gas interchange coefficient based on the surface of bubble by the flow-out of gas from cloud	[cm/sec]
k_{gd}	:	gas interchange coefficient based on the surface of bubble by diffusion	[cm/sec]
k_{gt}	:	total gas interchange coefficient based on the surface of bubble	[cm/sec]
l	:	distance between two sampling positions	[cm]
N_c	:	mass transfer rate from surface of cloud	[cm²/sec]
R	:	radius of cloud $\sqrt{(\alpha+1)/(\alpha-1)}\cdot a$	[cm]
r	:	polar co-ordinate in z plane	[cm]
s	:	co-ordinate defined in Fig. 5	[cm]
t	:	time	[sec]
u_0	:	u_{mf}/ε_{mf} interstitial gas velocity of continuous phase	[cm/sec]
u_{mf}	:	minimum fluidizing velocity	[cm/sec]

U_b	:	rising velocity of bubble	[cm/esc]
$\bar{U}_b$	:	average rising velocity of bubble	[cm/sec]
v_G	:	interstitial gas velocity along to stream line	[cm/sec]
x	:	rising direction of bubble	[cm]
y	:	direction perpendicular to x	[cm]
z	:	$= re^{i\theta}$	[cm]
α	:	U_b/u_0	[—]
β	:	polar co-ordinate in ζ plane	[rad.]
ε_{mf}	:	voidage fraction at minimum fluidization	[—]
ζ	:	$= \rho e^{i\beta}$	[cm]
θ	:	polar co-ordinate in z plane	[rad.]
λ	:	frequency of velocity and diameter of bubble of variation	[numbers/sec]
ρ	:	polar co-rodinate in ζ plane	[rad.]
ϕ_f	:	velocity potential	[cm²/sec]
ψ_f	:	stream function	[cm²/sec]

Literature cited

1) Kobayashi, H., Arai, F. and Sunakawa, T.: Kagaku Kogaku (Chem. Eng., Japan), **31**, 239 (1967)
2) Lewis, W.K., Gilliland, E.R. and Glass, W.: A.I.Ch.E. Journal, **5**, 419 (1959)
3) Szekely, J.: "Interaction between Fluids and Particles" (Instn. Chem. Engrs., London) p. 197 (1962)
4) Richardson, J.F. and Davies, L.: Trans. Isntn. Chem. Engrs., **44**, 293 (1966)
5) Rowe, P.N., Partridge, B.A. and Lyall, E.: Chem. Eng. Sci., **19**, 973 (1964)
6) Davidson, J.F. and Harrison, D.: "Fluidised Particles" Cambridge University Press (1963)
7) Muchi, I., Mori, Y. and Shichi, R.: The 4th General Symposium, (Society of Chemical Engineers, Japan) Tokyo, p. 31 (1965)